MULTIPACTING IN THE CRAB CAVITY

Y. Morita, K. Hara, K. Hosoyama, A. Kabe, Y. Kojima, H. Nakai, KEK, 1-1, Oho, Tsukuba, Ibaraki 305-0801, JAPAN
Md. M. Rahman, K. Nakanishi, Graduate University for Advanced Studies, 1-1, Oho, Tsukuba, Ibaraki 305-0801, JAPAN

Abstract

For the Research and Development of the crab cavity for KEKB, we have fabricated two prototype cavities. The crab cavity is a beam-deflecting cavity excited with the 508 MHz, TM110-like mode. To extract unwanted parasitic modes, the cavity has a squashed cell shape and a coaxial coupler along the beam pipe. The prototype cavities were tested in a vertical cryostat with/without the coaxial coupler. We observed multipacting at the first RF excitation. To study this event in detail, we measured temperatures of the coupler and cavity during RF tests. Temperature measurement showed that multipacting occurred at the tip of coaxial coupler at low RF fields, and then along the coaxial line. These events were processed in an hour. We observed another type of temperature rise around the iris. Temperature rise began at low fields, continued to rise up to a surface peak field of 18 MV/m, and then, disappeared above 20 MV/m. The excitation mode of the crab cavity has a maximum magnetic field and zero electric field on the same iris position. Temperature rise near this region suggests the multipacting events. A model simulation shows a stable two-point multipacting can exist at this position. We will present temperature measurement results and discuss multipacting near the iris.

INTRODUCTION

The crab cavity is a beam-deflecting cavity for the electron-positron collider accelerator with a finite angle beam crossing. Purpose of this cavity is to kick the beam bunch and to make head-on collision at the interaction region (crab crossing [1,2]). We started the R&D for a KEKB superconducting crab in 1994. This cavity has several unique characteristics [3]. The cavity has a squashed cell structure with a racetrack cross-section. The excitation mode is the TM110-like mode (crab mode, 508 MHz) that has magnetic fields perpendicular to the beam direction. To extract fundamental mode (TM010, 414 MHz) and parasitic higher order modes, a coaxial coupler structure is employed at the beam pipe. The cut-off frequency of the coupler was chosen to be 600 MHz, so the fundamental mode and higher order dipole modes can travel to downstream of the coupler, and then are absorbed by a RF absorber. The cavity is required to have high fields. Required kick voltage is 1.44 MV corresponding to the surface peak field of 21 MV/m. To establish fabrication and surface treatment techniques for the crab cavity, we have fabricated prototype cavities [4,5]. To test an influence of the coaxial coupler, we have made a short inner conductor made of Nb. The inner conductor was attached to the cavity beam pipe, and cavity performance was tested in a vertical cryostat [6,7]. The inner conductor caused the “Hydrogen Q-degradation”, however, quick cool-down procedure prevented this degradation, and we achieved required kick voltage [8].

At the first RF excitation of the cavity with the coaxial coupler, we observed multipacting event for about an hour. To study this event in detail, we measured temperatures of the inner conductor and the beam pipe of the coaxial structure. Heat creations at several positions were observed during multipacting processing. We also observed heat creations near the iris. Heat creations depended on the RF fields and disappeared at high fields. To identify the heating position, we measured temperatures of the cavity cell, especially around iris, and observed heat creations at several RF fields. Contrary to the accelerating cavities, the maximum surface magnetic field lies on the iris at the short axis of the cavity cell, while the electric field is zero at this position. Heat creation near this position suggests multipacting.

It is not so easy to simulate multipacting in the crab cavity, because there is no reliable method to calculate surface fields in three-dimensional, non-axially-symmetrical cavities. Therefore we consider a model that simulates multipacting near iris. The model shows that two-point multipacting can occur in the crab cavity near the iris.

VERTICAL COLD TESTS AND THE TEMPERATURE MEASUREMENT SYSTEM

The prototype cavity was installed in a vertical cryostat and cooled down with saturated liquid helium at 4.2 K. Fig. 1 shows a schematic figure of the cavity with dimensions in mm unit. The short inner conductor was attached to the small beam pipe (SBP). Inner pipe of the short conductor was terminated at a distance of 65 mm from the conductor tip. A vacuum port, an input coupler and a transmission coupler were set to the large beam pipe (LBP). These cavities were barrel-polished (>200 μm), electro-polished (100 μm), heat-treated at 700 °C for 3 hours, and rinsed with high-pressure ultra-pure water. Detailed description of surface treatments is found in Ref. 9.

Temperature sensors are 51Ω, 1/8W Allen-Bradley carbon resistors. These resisters are sustained on

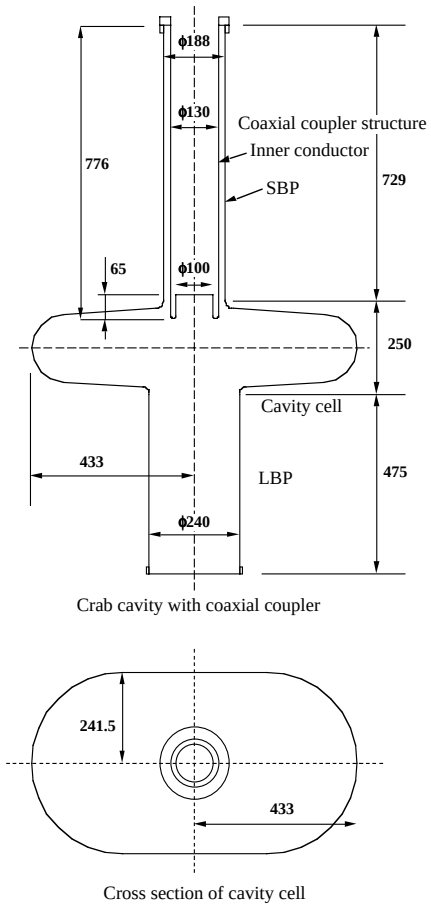

Figure 1: Crab cavity with coaxial coupler.

polyethylene terephthalate (PET) plates 0.5 mm thick. The PET plate has tension at 4.2 K so that the sensors are connected on the cavity surface. A FRP plate holds sensors and PET plate suspenders. Temperature sensors for the inner conductor tip are directly connected to FRP rod of diameter 2 mm. Fig. 2a shows a schematic figure of temperature sensors attached to the cavity surface. The sensor is connected to the 10V DC voltage source with a 1MΩ resister, and to DVM with multiplexer for sensor voltage measurement. Voltage measurement system is shown in Fig. 2b. Temperatures were calibrated at the end of each vertical cold test. The cryostat was evacuated from atmospheric pressure corresponding to saturated liquid helium temperatures from 4.2K to 4.0 K. Temperature T is given form the sensor resistance R as following fitting formula,

$$1/T = a + b \ln R,$$

where a and b are fitting parameters. Temperature rise of the cavity surface during RF test is given by extrapolating the fitting formula.

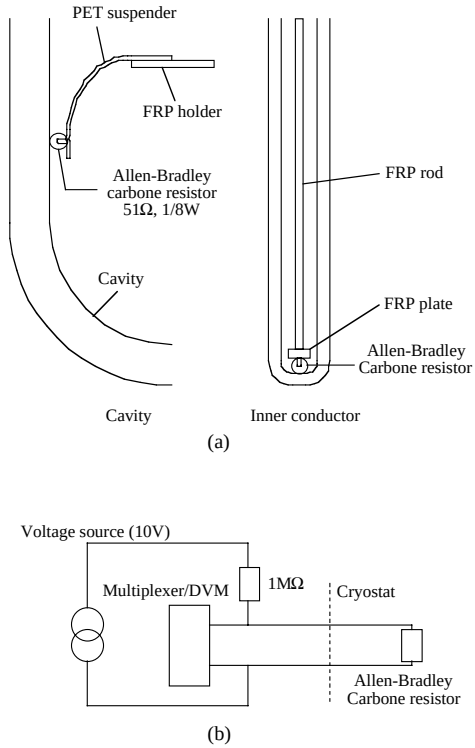

Figure 2: Temperature measurement system: (a) sensor and suspension, (b) voltage measurement system.

MEASUREMENT RESULTS

Prototype Cavity with the Coaxial Coupler

Prototype #1 cavity was tested with the coaxial coupler. To observe multipacting around coaxial coupler, 144 temperature sensors were attached surrounding SBP (5 layers) and at the tip of inner conductor (Fig. 3). SBP layers had the same angular distribution.

The cavity was excited with pulsed RF signal.

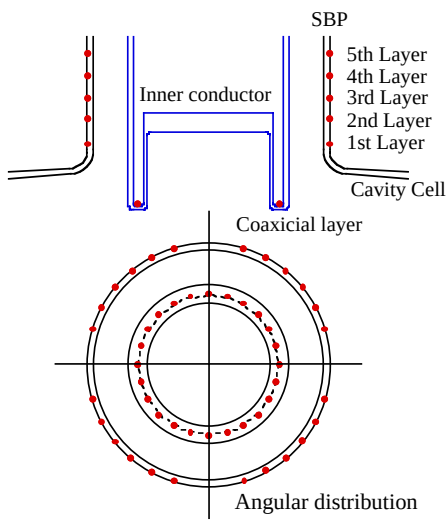

Figure 3: Temperature sensor layout.

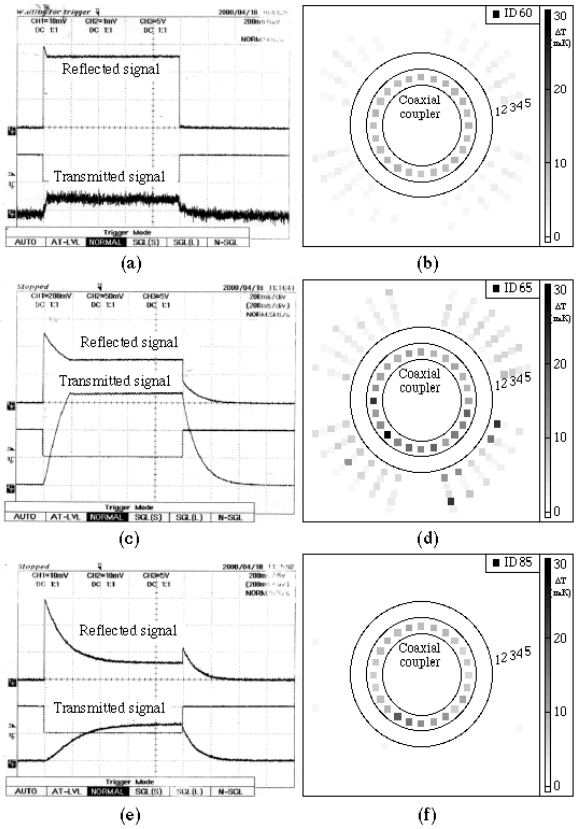

Figure 4: Reflected and transmitted signals during multipacting and corresponding temperature maps.

Transmitted and reflected signals showed typical form of multipacting (Fig. 4a). Temperature map is shown in Fig. 4b. Numbers in the map denote each SBP layer. Temperature rise at the tip of inner conductor was about 10 mK, while temperatures around SBP showed no significant rise. As this multipacting event was being processed (Fig. 4c), temperature rise around SBP began. Several heat spots appeared at the tip and around the SBP (Fig 4d). After an hour, the transmitted RF signal showed an end of multipacting (Fig. 4e), and SBP layers show no temperature rise (Fig. 4f). However, temperature rise at the tip still remained.

We also measured temperature rise during RF performance test. Qo curve as a function of surface peak field (Esp) is shown in Fig. 5a. Fig 5b and Fig. 5c show temperature map at 12 MV/m and mean temperatures of each layer as a function of Esp, respectively. Temperature rise at the tip was observed below 10 MV/m, while the first layer showed temperature rise between 12 and 19 MV/m. Mean temperatures from the first to fifth layers showed a temperature gradient. This gradient indicated that the heat creation occurred around the SBP iris.

Prototype Cavity without Coaxial Coupler

Above temperature measurement results suggest the multipacting occurs around SBP iris at several RF fields. We attached 264 temperature sensors to cover around the SBP and LBP irises. Sensor layout is shown in Fig. 6. The SBP half-cell has first layer, second layer, a SBP iris layer,

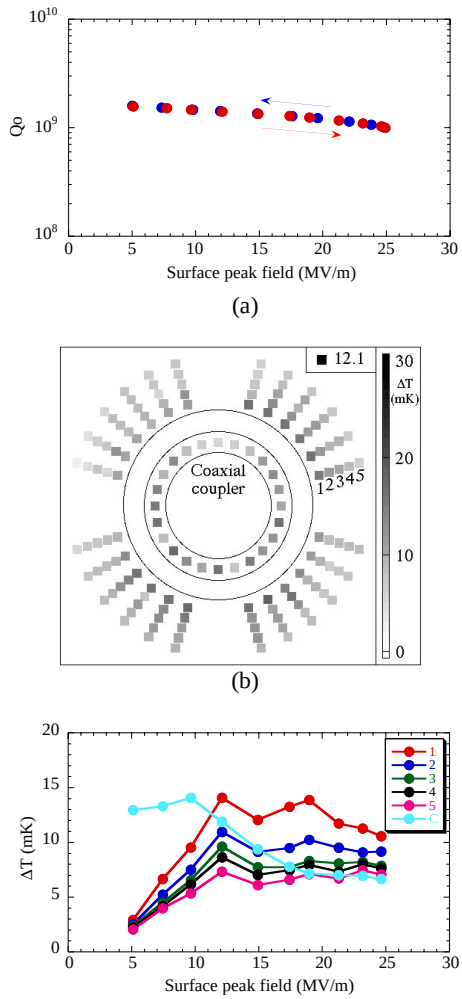

Figure 5: Temperature rise during RF excitation: (a) Qo curve, (b) temperature map at 12 MV/m, (c) mean temperatures of each layer as a function of Esp. Numbers denote each SBP layer and C denotes the coaxial layer.

a 240ϕ layer, and a 300ϕ layer (red circles), and a flat region layer (blue circles). The first, second, and SBP layers have the same angular distribution. The LBP half-cell has a LBP iris layer (red circles) and a flat region layer (blue circles). The cold-tested cavity is the prototype #2 without the inner conductor. Fig. 7a shows a Qo curve at the first RF excitation. Fig. 7b is a temperature map at 12 MV/m. There were several heat spots in the LBP half-cell at low fields (black circles in Fig. 7b). These spots were processed at 16 MV/m and never reappeared. As the RF field was raised, temperature rise around SBP iris began. This rise continued up to 12 MV/m, and then disappeared above 15 MV/m. Fig. 7c shows the typical temperature curves at the 240ϕ layer. Line colours represent temperatures at the position with the same colour circles in Fig 7b. X-ray radiation began at 15 MV/m and Qo gradually decreased. At 26 MV/m, X-ray radiation intensity decreased, and the RF fields reached

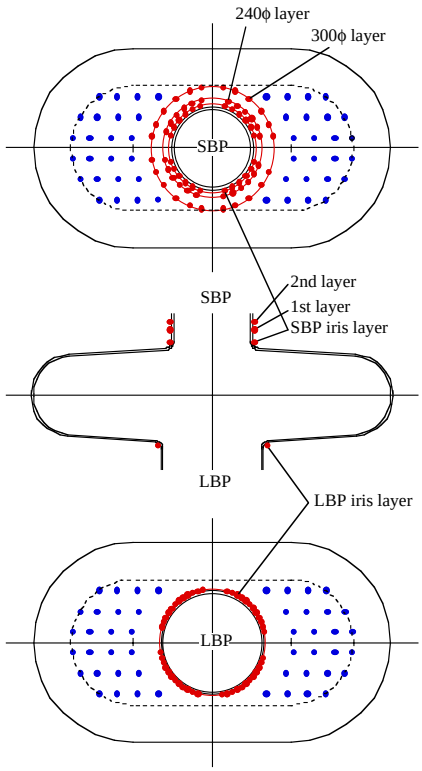

Figure 6: Temperature sensor layout. Red dots denote layers near the iris and blue dots denote flat region layers.

33 MV/m. The radiation intensity was detected by several Pin-diodes attached on the cavity surface. Finally the RF field reached to 34 MV/m. The field limitation was due to the RF power source. As the RF field decreased, temperature rise around SBP iris reappeared at 18 MV/m. There were two types of heat creations around SBP iris. One is heat creation at 12 MV/m, and the other is at 18 MV/m.

Qo curve during the second RF excitation are shown in Fig. 8a. Fig. 8b shows a temperature map at Esp of 18 MV/m. Heat spots in the LBP half-cell disappeared as shown in Fig. 8b. Fig. 8c shows temperature curves at the 240ϕ layer. Temperature rise around SBP iris continued up to 18 MV/m, then disappeared above 20 MV/m. No temperature rise was observed as the RF field decreased. Once heat creation at 18 MV/m was activated, it always appeared in the RF excitations.

MODEL SIMULATION

To identify these heat creations with multipacting, numerical simulation is needed. However, there is no reliable calculation method to give surface fields of the crab cavity. Therefore we estimated surface fields around the iris using MAFIA computer code. Calculated fields near cavity surface usually have large errors depending on the mesh assignments. Several calculated fields near the surface boundary are neglected. Surface fields were given by extrapolating calculated fields to the cavity boundary.

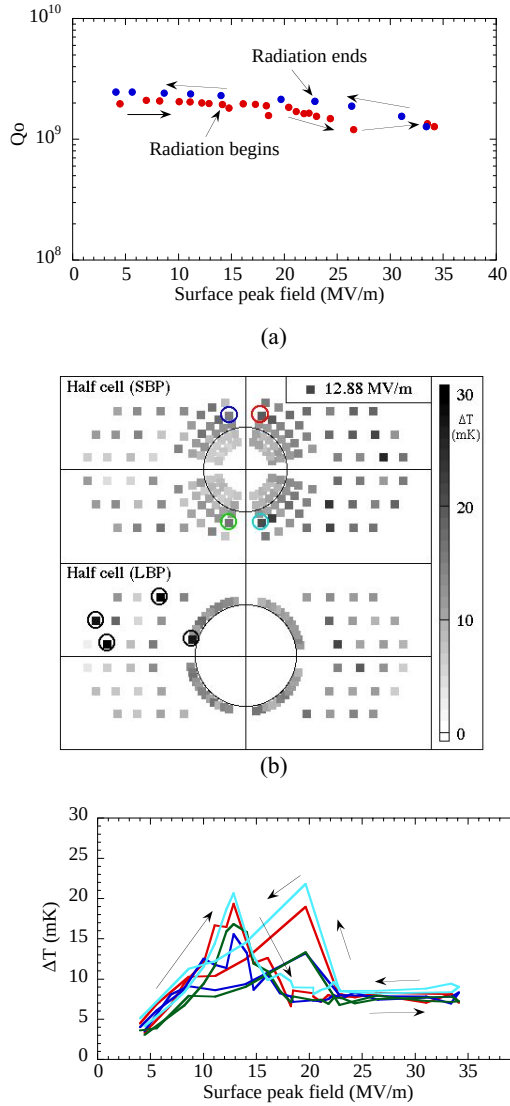

Figure 7: Temperature rise during the first RF excitation: (a) Qo curve, (b) temperature map at 13 MV/m, (c) temperature curves as a function of Esp. Line colors denote positions in (b).

Using this method, magnetic surface fields Bs were calculated from the SBP iris to the 240ϕ layer. The peak magnetic field in the SBP half-cell lies on the iris at the short axis and the surface fields largely change from the iris to the 240ϕ layer. At the peak electric field of 12 MV/m, calculated surface magnetic fields range from 138 to 250 G. These fields are comparable with the resonant field for the one-point multipacting of first-order. Resonant field B is given by,

$$B = \frac{1}{n}\varepsilon\frac{m}{e}\omega,$$

where n is the order of multipacting, m is the electron mass, e is the electron charge, ω is RF frequency, and ε is around 0.64 for pillbox-type cavities [10]. Product of

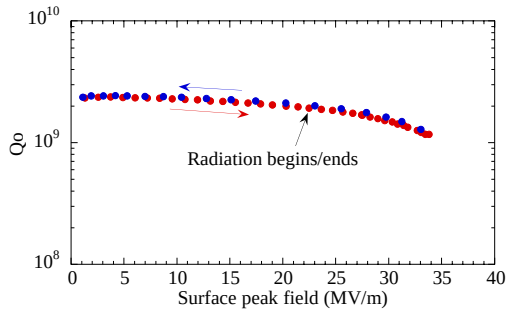

(a)

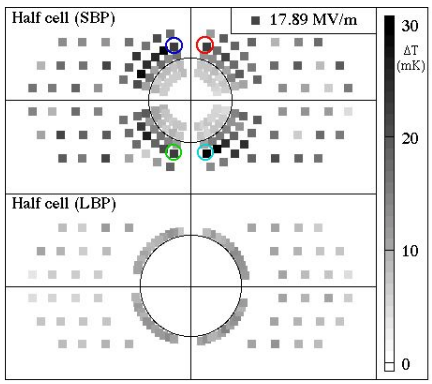

(b)

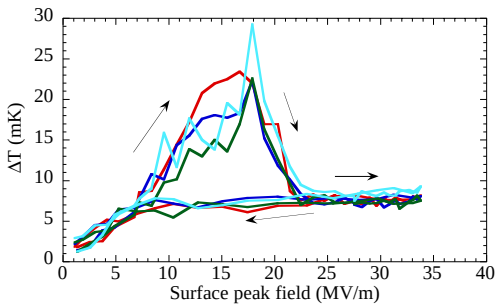

(c)

Figure 8: Temperature rise during the second RF excitation; (a) Qo curve, (b) temperature map at 18 MV/m, (c) temperature curves as a function of Esp. Line colors denote positions in (b).

ωm/e gives magnetic field of 180 G. Heat creation at 12 MV/m suggests the one-point multipacting of first order. On the other hand, calculated surface magnetic fields range from 208 to 375 G at the peak field of 18 MV/m. The fields are above the resonant field with n=1. Two-point multipacting should be considered.

Although three-dimensional numerical simulation in the crab cavity is difficult, one can consider a two-dimensional model that reproduces two-point multipacting near iris. We assumed constant magnetic field over the flat surface and electric field with uniform gradient. A stable two-point multipacting trajectory exists in this field configuration. Fig. 9 shows an example of stable trajectory. We assumed that the incident electron energy is 2 eV [11,12], and only one secondary electron is

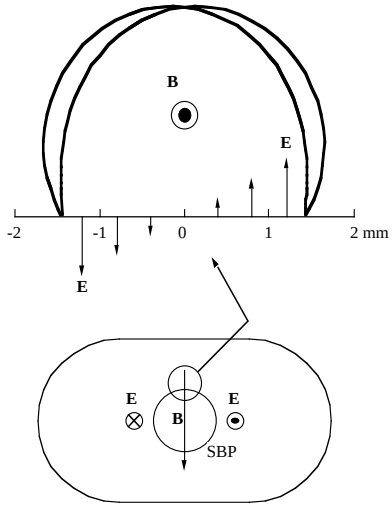

Figure 9: Stable trajectory and field configuration used in the model.

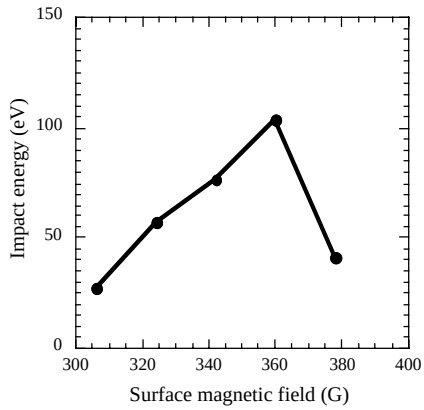

Figure 10: Impact energy as a function of surface magnetic field.

emitted normal to the surface with 2 eV. The constant magnetic field is 360 G, that is, the resonant field of the two point multipacting of first order (n=1/2). Fig. 10 shows electron impact energy as a function of constant magnetic field. The electric field gradient is 76 MV/m^2. Below 300 G, or above 380 G, impact energy becomes too small (< 20 eV) for secondary electron emission. The gradient of electric field is an important parameter. The gradient should be in the range from 65 to 85 MV/m^2. Electric field calculation near the iris at the short axis results the field gradient about 80 MV/m^2 that is within the range for the stable trajectory. This model suggests the two-point multipacting of first order near the iris at 18 MV/m.

The surface field calculation indicates that the LBP iris has the same condition for the tow-point multipacting as for the SBP iris. It is very natural that the LBP iris has heat creations by this type of multipacting. However, we observed no significant heat creations around this region.

CONCLUSION

We have measured temperatures of the prototype cavities during RF tests. Multipacting event was observed at the first RF excitation. Multipacting at the tip of inner conductor began first. As this multipacting was being processed, multipacting along the coaxial line began. This event was processed in an hour and multipacting along the coaxial line was not observed after the processing. The tip of inner conductor showed heat creations below the peak field of 10 MV/m.

We observed heat creations near the iris. There were two types of heat creation. One is at 12 MV/m and the other is at 18 MV/m. Surface field estimation suggests the one-point multipacting of first order at 12 MV/m. A model simulation, which assumes a flat surface, constant magnetic field, and electric field with uniform gradient, suggests the two-point multipacting of first order (n=1/2) at 18 MV/m. This type of heat creation did not always appear during RF tests, however, once activated, it always appeared. Further studies are needed to definitely identify heat creations at several fields with multipacting event.

Finally, these heat creations do not limit the cavity performance and disappear above 20 MV/m.

REFERENCES

[1] R. B. Palmer, SLAC-PUB 4707 (1988).
[2] K. Oide and K. Yokoya, Phys. Rev. A40, p. 315 (1989).
[3] K. Akai et al, Proc. IEEE Part. Accel. Conf., p. 757 (1993).
[4] K. Hosoyama et al, Proc. of the 7th Workshop on RF Superconductivity, p. 671 (1995).
[5] K. Hosoyama et al, Proc. of the 8th Workshop on RF Superconductivity, p. 547 (1997).
[6] K. Hosoyama et al, Proc. of the 1st APAC, p. 828 (1998).
[7] H. Nakai et al, Advances in Cryogenic Engineering, Vol. 45, p. 853 (2000).
[8] Y. Morita et al, Proc. of the 10th Workshop on RF Superconductivity, p. 403 (2001).
[9] H. Nakai et al, paper presented at this conf.
[10] H. Piel, Superconductivity in Particle Accelerators, p. 149, CERN 89-04.
[11] W. Weingarten, Proc. of the 2nd Workshop on RF Superconductivity, p. 551 (1984).
[12] J. Knobloch et al, Proc. of the 8th Workshop on RF Superconductivity, p. 1017 (1997).